Jpn. J. Appl. Phys. Vol. 35 (1996) pp. 3904–3908
Part 1, No. 7, July 1996

Optical Properties of Er-Doped $CuAlS_2$

Yasukazu KIMURA*[1], Tsuyoshi OHGOH*[2], Igor AKSENOV*[3] and Katsuaki SATO*[4]
Faculty of Technology, Tokyo University of Agriculture and Technology, Koganei, Tokyo 184, Japan

(Received November 14, 1995; accepted for publication April 26, 1996)

Photoluminescence (PL) spectra of Er-doped $CuAlS_2$ single crystals grown by the chemical vapor transport technique were studied for the first time. Two kinds of crystals were prepared under different doping conditions, i.e., one was doped with Er alone (type I crystals) and the other were doped with Er and a very small amount of Fe (type II crystals). PL spectra of both type I and type II crystals showed three sharp emissions, at 2.34 eV (A-emission), 2.26 eV (B-emission) and 1.85 eV (C-emission), which were attributed to $^2H_{11/2} \rightarrow {}^4I_{15/2}$, $^4S_{3/2} \rightarrow {}^4I_{15/2}$ and $^4F_{9/2} \rightarrow {}^4I_{15/2}$ f-f transitions of Er^{3+} ions, respectively. The intensity of f-f emisions in type II crystals was substantially larger than that in type I crystals. The emission peak at 2.34 eV (A-emission) has an excitation band at 3.24 eV, which is assigned to $^4I_{15/2} \rightarrow {}^4G_{11/2}$ transitions of Er^{3+} ions on the Dieke diagram. In addition to the Er-related f-f emissions, a broad yellow-orange emission band was observed in both crystals at low temperatures. The yellow-orange emission dominated the room-temperature (RT) emission spectra of type I crystals, whereas the emission was almost quenched at RT in the case of type II crystals. The enhancement of Er-related emission and the quenching of the yellow-orange emission due to the presence of Fe impurity are discussed in terms of the site preference and the charge neutrality requirement.

KEYWORDS: $CuAlS_2$ ternary semiconductor, Er rare earth ion, Fe impurity, f-f transition, photoluminescence, photoluminescence excitation

1. Introduction

Semiconductors doped with rare-earth (RE) elements have been attracting interest as materials for full-color electroluminescent devices,[1] because the RE ions become luminescent centers with narrow line-width emissions resulting from electronic transitions between the L-S coupling terms of 4f-shell related multiplets (so-called f-f transitions) associated with $4f^n$ states of RE ions.

The chalcopyrite-type semiconductor $CuAlS_2$, which is the widest band-gap member of the I–III–VI_2 family, has a direct energy gap of about 3.55 eV at 10 K,[2] which is wide enough to accommodate the RE-related luminescent centers emitting in the visible spectral region. Since $CuAlS_2$ contains both monovalent (Cu) and trivalent (Al) cations, it is possible for trivalent RE ions to occupy both Cu and Al sites in the host lattice. However, the substitution of Cu and Al in the $CuAlS_2$ host lattice with trivalent RE ions is difficult in both cases, since (1) substitution of monovalent Cu results in violation of the charge neutrality condition and, therefore, must be accompanied by the formation of intrinsic defects, which compensate the excess charge in the lattice, whereas (2) substitution of the trivalent Al is difficult due to the small radius of an Al ion (~ 0.53 Å) compared with that of RE ions (~ 1 Å). For this reason the actual (verified by EPMA analysis) concentration of RE elements in $CuAlS_2$ is usually much lower than the concentration of these elements in a starting mixture of constituent elements.[3]

We previously reported observing sharp emissions due to f-f transitions of trivalent Tb,[4] Tm[3] and Ho[5] ions in the $CuAlS_2$ host lattice. However, all the previously reported sharp RE-ion-related emissions in $CuAlS_2$ were observed as being superposed on a broad yellow-orange emission occurring as a result of defects or impurities inherent to the host material.

In this paper we report results of optical studies on Er-doped $CuAlS_2$ crystals, in which a series of sharp Er^{3+}-related emissions were observed, and show that the broad yellow-orange emission can be suppressed by doping with Fe as a coactivator, which transforms the material into a green-emitting phosphor.

2. Experimental

Er-doped $CuAlS_2$ crystals were grown by chemical vapor transport (CVT) technique from two different starting materials. In the first case, the starting material was composed of $CuAlS_2$ powder, which had been prepared by directly melting the constituent elements,[6] and the elemental Er metal, with a molar ratio of $CuAlS_2$ vs. Er of 0.95 : 0.05 (type I crystals). In the second case, crystal growth was carried out using the constituent elements to achieve a molar ratio of Cu : Er : Al : Fe : S = 0.95 : 0.05 : 0.9995 : 0.0005 : 2.0 (type II crystals). In the latter case, we aimed at doping Er into the Cu sites in the chalcopyrite lattice, in order to introduce $[Er^{3+}]_{Cu+}$ defects capable of acting as donor states in the semiconductor. On the other hand, Fe were added into the type II crystals to compensate for the lack of charge neutrality resulting from the $[Er^{3+}]_{Cu+}$ state, by changing the valence of the Fe ion occupying the Al site ($[Fe]_{Al}$) from trivalent to divalent. Here we assumed a priori that most of the Fe impurities occupy Al sites, taking into account the existence of a mineral $CuFeS_2$, that is regarded as 100% substitution of Fe in $CuAl_{1-x}Fe_xS_2$ system.

The starting materials were sealed in an evacuated silica ampoule with an inner diameter of 13 mm and 200 mm in length together with iodine, the concentra-

*[1]Present address: Mobara Works, Hitachi Ltd., Mobara, Chiba 297, Japan.
*[2]Present address: Fuji Photo Film Co., Ltd., Kaisei-machi, Kanagawa 258, Japan.
*[3]Present address: Electrotechnical Laboratory, Umezono, Tsukuba 305, Japan.
*[4]To whom reprints requests should be addressed.

tion of which was 10 mg/cm^3 of the inner volume of the ampoule. The ampoule was placed in a two-zone furnace and the transport was carried out for seven days while the temperature of the source zone was gradually raised from 750°C to 900° C and that of the growth zone from 600°C to 750°C. The resulting crystals were translucent blue (type I crystals) or yellow (type II crystals) with typical dimensions of 0.513 mm^3 and exhibited a well-developed {112} crystal plane.

Optical absorption spectra for photon energies between 1.4 and 3.5 eV were measured at room temperature (RT) using a Hitachi U-3410 spectrophotometer. Infrared absorption spectra between 2000 and 6000 cm^{-1} were measured using a BOMEM-type MB100 Fourier Transform Infrared (FTIR) spectrometer. Photoluminescence (PL) measurements were carried out using the 365 nm line of a super high-pressure Hg lamp, with the samples placed in an Oxford Instruments CF1104 cryostat evacuated to about 10^{-6} Torr. The emitted light was dispersed by a JASCO CT-25C monochromator and detected by a Hamamatsu R928 photomultiplier. For PL excitation (PLE) measurements, a 150W Xe lamp combined with a JASCO CT-25A monochromator was used as an excitation source, the emitted light being dispersed by a JASCO CT-25C monochromator and detected by a Hamamatsu R928 photomultiplier. Correction of the spectral response of the detection system was carried out for all the spectra obtained.

3. Results and Discussion

3.1 *Er^{3+}-related emissions*

Figures 1(a) and 1(b) show temperature dependence of typical PL spectra for the type I and type II crystals of Er-doped $CuAlS_2$, respectively. The vertical axis is scaled using arbitrary units. To indicate the relative intensity of the different spectra we give a multiplication factor beside each spectral curve, the standard of which is the 70 K spectrum for the type II crystal (Fig. 1(b)).

The spectra commonly exhibit a series of three sharp emission lines with peaks at 2.34 eV (A-emission), 2.26 eV (B-emission) and 1.85 eV (C-emission), which are considered to be associated with f-f transitions in Er^{3+}. These emission lines are superposed on a broad yellow-orange emission band which will be discussed in §3.3. The intensity of the B-emission showed little temperature dependence, while that of A- and C-emissions showed relatively strong temperature dependence. The intensity of A-, B- and C-emissions in type II crystals is approximately one order of magnitude larger than that in type I crystals. The A- and B-emissions in both types of crystals show fine structures as illustrated in Fig. 2.

All of the sharp emissions can be attributed to the f-f transitions in Er^{3+} ions having $4f^{11}$ electronic configuration. It is widely accepted that the electrons of the 4f-shell are screened from the surrounding ligands of the host crystal lattice by diffuse outer electron shells, which

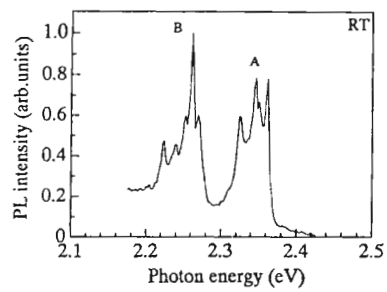

Fig. 2. Fine structures in A- and B-emissions of Er-doped $CuAlS_2$ single crystal of type I. The similar fine structures were observed in type II crystals.

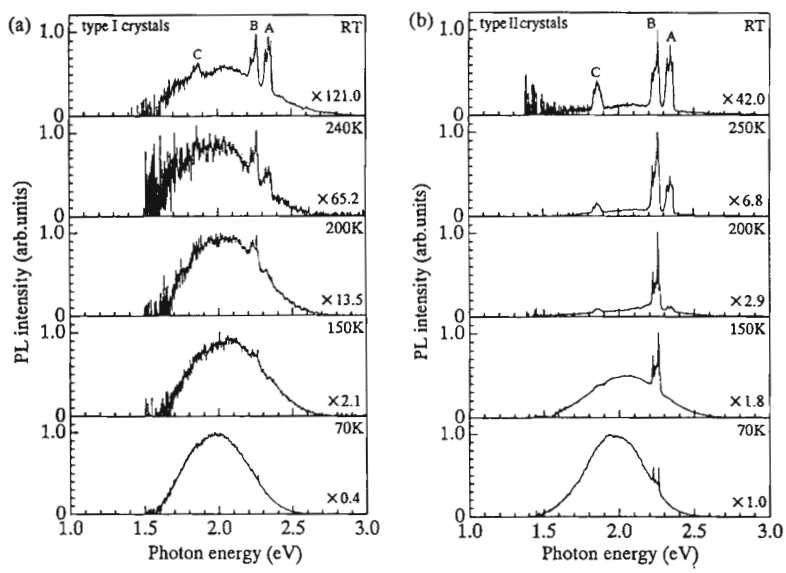

Fig. 1. PL spectra for (a) type I and (b) type II single crystals of Er-doped $CuAlS_2$ measured at different temperatures.

results in (1) very weak interaction of the 4f-electrons with vibrational modes leading to the observation of the sharp emissions even at room temperature and (2) very weak interaction of the 4f-electrons, with ligand field splitting smaller than spin-orbit splitting. We therefore expect that the spectral positions of the f-f optical transitions of the ions will not show a drastic dependence on the materials nor on the crystal lattice sites which Er^{3+} ions occupy. Therefore, we can use the Dieke diagram shown in Fig. 3 for RE elements[7] to attribute the observed emissions to the f-f transitions of Er^{3+} ions.

As a result A-, B- and C-emissions were assigned to the f-f transitions from the excited multiplets $^2H_{11/2}$, $^4S_{3/2}$ and $^4F_{9/2}$ to the ground multiplet $^4I_{15/2}$ as shown by arrows A, B and C in the energy diagram shown in Fig. 3. It should be noted that the spectral positions of these emissions are very close to those observed for Er-doped ZnS,[8] which is a binary analog of $CuAlS_2$. In the case of the Er-doped $CuAlS_2$, however, the emissions are split into fine structures consisting of a series of very sharp lines (shown in Fig. 2 for A- and B-emissions). The fine structures may be caused by the non-cubic component of the ligand field in the crystal lattice of $CuAlS_2$ with tetragonal symmetry, detailed analysis of which is planned for future studies.

As described previously, the temperature dependence of the emission intensity differs between the B-line, and the A- and C-lines. A similar tendency in temperature dependence among f-f transitions was observed for Er-doped ZnS.[9] To elucidate the reason we measured PLE spectra of these emission lines. We succeeded in obtaining PLE spectra for both A- and B-emissions in type II crystals, while we failed to observe PLE for the B-emission in type I crystals presumably due to the low intensity of the emission. The PLE spectra for the A-emission in type I and those for A-, B-emissions in type II crystals are given in Figs. 4(a) and 4(b), respectively.

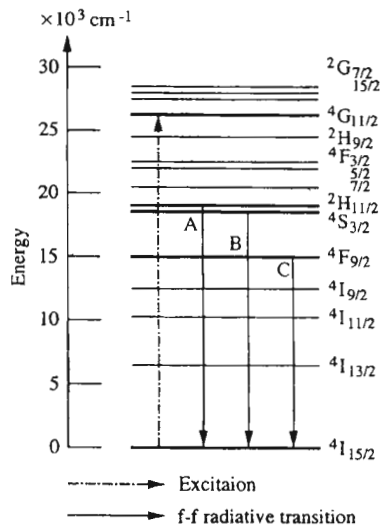

Fig. 3. Dieke diagram for energy levels of $4f^{11}$ multiplets of Er^{3+} ion.

The PLE spectrum of A-emission (2.34 eV) in the type II crystal exhibits a sharp line with a full width at half-maximum (FWHM) of $\sim 400\,cm^{-1}$ at 3.24 eV and a broad excitation band just below the band edge (peak at 3.32 eV), while that of B-emission (2.26 eV) has no PLE peak at 3.24 eV but shows the same broad excitation band (3.32 eV) as observed for A-emission. Since the energy (3.24 eV) of the sharp PLE peak corresponds to the transition energy of $^4I_{15/2} \rightarrow {}^4G_{11/2}$ on the Dieke diagram shown in Fig. 3, the excited electronic state relaxes through a radiative or non-radiative process to the lower excited state $^2H_{11/2}$, which in turn relaxes to the ground state $^4G_{11/2}$,with emission of the 2.34 eV photon (A peak).

On the other hand, the B-emission did not occur due to the same $^4I_{15/2} \rightarrow {}^4G_{11/2}$ transition. Generally speaking, both A- and B-transitions should share the same PLE spectrum, since the two excited multiplets $^2H_{11/2}$ (excited state of A-emission) and $^4S_{3/2}$ (excited state of B-emission) have an energy difference as small as 80 meV and can be considered to be in thermal equilibrium. Nevertheless, A- and B-emissions do not share a common excitation spectrum, suggesting that different excitation mechanisms are involved.

Let us recall that both $^4I_{15/2} \rightarrow {}^2H_{11/2}$ and $^2H_{11/2} \rightarrow {}^4G_{11/2}$ transitions should be accompanied by a change of spin quantum number by -1 and $+1$, respectively, if electric dipole transition is assumed. The spin quantum number can only be conserved if the two transitions occur simultaneously. We believe that this is the case for A-emission. In contrast, no such simultaneous transition occurs for transition $^4S_{3/2} \rightarrow {}^4G_{11/2}$ (B-emission), since spin is conserved in this process.

Another possible explanation for the different PLE

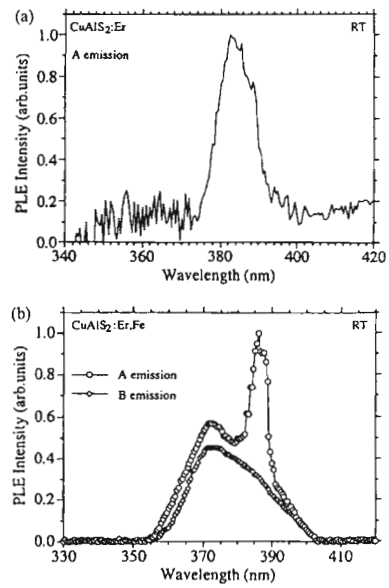

Fig. 4. Photoluminescence excitation (PLE) spectra of (a) A-emission in a type I crystal and (b) A- and B-emission in a type II crystal.

spectra for A- and B-emssions is that these emissions originate from different Er centers; for example, one is from an Er ion that substitutes for Cu or Al site and the other from an Er ion that occupies the interstitial site, and selection rules differ between the two centers. Further studies are necessary to clarify both the temperature dependence and the PLE mechanism.

By comparison of Figs. 1(a) and 1(b), we find that the intensity of the Er^{3+}-related f-f emissions of type II crystals is comparatively stronger than that of type I crystals. We believe that the difference is caused by the increased concentration of Er^{3+} centers in type II crystals. In type I crystals, Er^{3+} ions are thought to occupy Al^{3+} sites, forming the isoelectronic centers. However, as described in §1, the substitution of Er^{3+} into the Al^{3+} site in the $CuAlS_2$ host lattice is difficult due to the small radius of an Al^{3+} ion. If we aim at increasing the Er concentration in $CuAlS_2$, we should ensure that Er ions occupy Cu-sites, the ionic radius of which is comparable to the radius of Er^{3+}.

Therefore, in type II crystals, due to appropriate adjustment of the starting composition, Er^{3+} ions were expected to preferentially occupy Cu^{+} sites. In addition, the violation of charge neutrality introduced by the $[Er^{3+}]_{Cu^{+}}$ center was expected to be compensated by the change of the valence of Fe occupying the Al sites.

3.2 *Yellow-orange emission band*

The broad yellow-orange emission dominates the low-temperature spectra of both type I and type II crystals. The intensity of the yellow-orange emission decreases with increase of temperature, while that of f-f transitions of Er^{3+} shows no drastic change. This is the reason why Er-related emissions are clearly observable at elevated temperatures. The intensity of the broad yellow-orange emission relative to that of Er-related emissions is much higher in type I crystals than in type II crystals over the whole temperature range.

The intensity of the broad yellow-orange emission remains dominant at RT in type I crystals, by which the observed emission of the type I crystals looks yellow-orange in color at RT, whereas for type II crystals the yellow-orange emission is almost quenched at RT, resulting in the observation of a "pure" series of Er^{3+}-related sharp emissions. At RT the observed emission of type II crystals was green instead of the yellow-orange for the type I crystals. Addition of a small amount of Fe impurities was thus found to play a crucial role in the quenching of the yellow-orange emission, since crystals formed from the starting material with a composition of Cu : Er : Al : S = 0.95 : 0.05 : 1.0 : 2.0, without addition of Fe impurities, always showed bright yellow-orange emissions.

Such a yellow-orange emission has commonly been observed in iodine-transport single crystals with or without RE elements. Time-resolved spectra revealed that the emission is of donor-acceptor pair type.[4] Several mechanisms have been proposed for the broad yellow-orange emission. One involves intrinsic defects, such as vacancies, anti-sites or a complex defect. Another is associated with impurities, particularly transition elements, which occupy cation sites (Cu or Al) substitutionally, or interstitial sites, sometimes forming a complex with other defects or impurities. The role of the Fe impurity in reducing the intensity of the broad yellow-orange band may be different depending on what sort of mechanism is involved in the emission. The electronic states of Fe will be discussed in the next subsection in connection with optical absorption spectra.

3.3 *Absorption spectra of iron impurities in Er-doped crystals*

The optical absorption spectra of Er-doped crystals between 1.4 and 3.5 eV are shown in Fig. 5. The spectrum of type II crystals exhibits a broad absorption A-band at about 2.9 eV, whereas that of type I crystals shows a broad absorption B-band at 1.9 eV. The B-band was previously observed in undoped and Fe-doped $CuAlS_2$ crystals and has been assigned, on the basis of the results of optical and ESR studies, to the charge transfer transitions from the valence band to the 3d-shell-related orbitals of Fe^{3+} impurities occupying Al^{3+} sites in the host crystal lattice.[10,11]

The quenching of the Fe^{3+}-related absorption B-band in type II crystals can be explained by the upward shift of the Fermi level in type II crystals from its position in type I crystals. The result of this shift leads to the capture of electrons from the valence band on Fe^{3+} impurities with the subsequent change in the valence state of Fe^{3+} resulting in the formation of Fe^{2+}.

More evidence of the presence of Fe^{2+} impurities in type II crystals is provided by the FTIR absorption spectra shown in Fig. 6. While the spectra of type I crystals show no remarkable features in the measured infrared (IR) spectral range, those of type II crystals exhibit two broad IR absorption band peaks at about 3400 cm^{-1} (0.42 eV) and 4300 cm^{-1} (0.53 eV).

Since the spectral positions of these IR absorptions agree well with the predicted energy of the lowest excited state of an Fe^{2+} ion occupying an Al site in $CuAlS_2$, as estimated from the ESR studies,[12] we attribute the IR absorptions, observed in type II crystals, to $^5B_1$ (^5E) → $^5B_2$ ($^5T_2$) and $^5B_1$ (^5E) → ^5E ($^5T_2$) electronic transitions within the 3d-shell-related orbitals of the divalent irons on Al sites. (Notations in the parenthesis are the irreducible representations in T_d symmetry from which

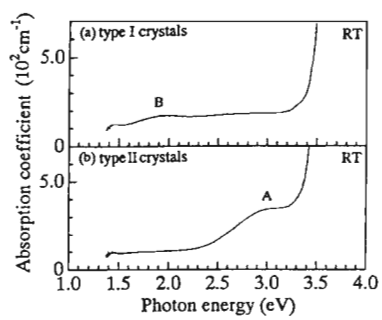

Fig. 5. Optical absorption spectra between 1.4 and 3.5 eV for (a) type I and (b) type II single crystals of Er-doped $CuAlS_2$.

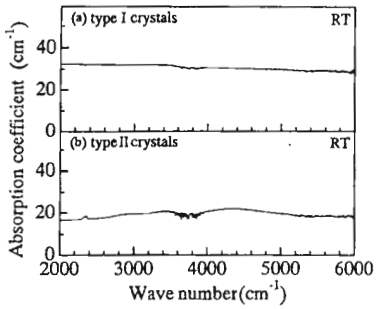

Fig. 6. Infrared absorption spectra for (a) type I and (b) type II single crystals of Er-doped $CuAlS_2$.

D_{2d} symmetry is derived.) Similar IR absorptions have been observed in $CuGaS_2$ (4000 cm^{-1}), $CuInS_2$ (3200 and 3900 cm^{-1}) and $CuInSe_2$ (3300 cm^{-1}) and have been attributed to the d-d crystal field transitions in Fe^{2+} ions in D_{2d} symmetry.[13]

More evidence of the presence of Fe^{2+} is provided by the absorption spectrum of type II crystals between 1.4 and 3.5 eV shown in Fig. 5(b). The broad A-band absorption observed around 2.9 eV has also been observed in ZnS:Fe, which was attributed to higher excited states derived from ^3P, ^3H, ^3F and ^3G of free Fe^{2+} ions.[14]

3.4 *PL properties in Er-doped and Er, Fe-doped $CuAlS_2$*

We believe that in type I crystals Er ions primarily occupy Al sites in the crystal lattice with the formation of the $[Er^{3+}]_{Al^{3+}}$ defects, which are isoelectronic centers and do not influence the Fermi level position. Therefore the Fermi level position in type I crystals may stay below the Fe^{2+}/Fe^{3+} demarcation level for the Fe_{Al} defect, leading to the observation of the absorption band B (1.9 eV) ascribed to Fe^{3+}.

On the other hand, Fe was detected as a $[Fe^{2+}]_{Al^{3+}}$ defect in type II crystals in optical spectra as shown in the previous subsection. The experimental evidence strongly supports the hypothesis that Er ions primarily occupy Cu sites in the crystal lattice and form $[Er^{3+}]_{Cu^+}$ defects.

The observed reduction of the broad yellow-orange emission in type II crystal may be related to the presence of divalent Fe occupying the Al site. The excitation energy of the broad yellow-orange emission, regardless of its origin, may be transferred to the $[Fe^{2+}]_{Al}$ center, where a nonradiative recombination or an infrared emission occurs. Further studies are necessary to clarify whether or not such an energy transfer in fact occurs.

4. Conclusion

The PL spectra of $CuAlS_2$ crystals doped with Er under two different doping conditions showed three sharp emission lines, at 2.34 eV (A-emission), 2.26 eV (B-emission) and 1.85 eV (C-emission), which were assigned to the electronic transitions between the multiplets in $4f^{11}$ configuration of Er^{3+} ion, i.e., $^2H_{11/2} \rightarrow {}^4I_{15/2}$, $^4S_{3/2} \rightarrow {}^4I_{15/2}$ and $^4F_{9/2} \rightarrow {}^4I_{15/2}$, respectively. The A- and B-emissions not only showed different temperature dependences but also had different excitation spectra. A difference in excitation mechanism between A- and B-emissions was suggested.

The broad yellow-orange emission band related to the host material dominated the Er-related green PL spectrum of type I crystals, in which Er ions are believed to occupy Al sites. On the other hand, in type II crystals in which Er ions occupy Cu sites, the broad yellow orange emission was found to be quenched at RT, making the emission green. We conclude that the addition of a small amount of Fe impurities plays an important role in quenching of the yellow-orange emission in type II crystals.

1) T. Suyama, N. Sawara, K. Okamoto and Y. Hamakawa: *Proc. 13th Int. Conf. Solid State Devices, Tokyo, 1981*, Jpn. J. Appl. Phys. **21** (1982) Suppl. 21-1, p. 383.
2) S. Shirakata, I. Aksenov, K. Sato and S. Isomura: Jpn. J. Appl. Phys. **31** (1992) L1071.
3) T. Ohgoh, I. Aksenov, Y. Kudo and K. Sato: Jpn. J. Appl. Phys. **33** (1994) 962.
4) Y. Kudo, N. Kojima, Y. Takada, I. Aksenov and K. Sato: Jpn. J. Appl. Phys. **31** (1992) L663.
5) T. Ohgoh, Y. Kudo and K. Sato: *Proc. 9th Int. Conf. Ternary and Multinary Compounds, Yokohama, 1993*, Jpn. J. Appl. Phys. **32** (1994) Suppl. 32-1, p. 608.
6) I. Aksenov, Y. Kudo and K. Sato: Jpn. J. Appl. Phys. **31** (1992) L145.
7) G. H. Dieke and H. M. Grosswhite: Appl. Opt. **2** (1963) 675.
8) E. W. Chase, R. T. Hepplewhite, D. C. Krupka and D. Kahng: J. Appl. Phys. **40** (1969) 2512.
9) S. Larach, R.E. Shracler and P.N. Yocom: J. Electrochem. Soc. **116** (1969) 471.
10) I. Aksenov and K. Sato: Jpn. J. Appl. Phys. **31** (1992) 2352.
11) K. Sato, I. Aksenov, N. Nishikawa and T. Kai: *Proc. 9th Int. Conf. Ternary and Multinary Compounds, Yokohama, 1993*, Jpn. J. Appl. Phys. **32** (1994) Suppl. 32-1, p. 481.
12) U. Kaufmann: Solid State Commun. **19** (1976) 213.
13) K. Sato, I. Aksenov, N. Nishikawa, T. Shinzato and H. Nakanishi: to be published in *Proc. 10th Int. Conf. Ternary and Multinary Compounds, Stuttgart, September 1995*, J. Cryst. Res. & Technol.
14) G.A. Slack, F.S. Ham and R.M. Chrenko: Phys. Rev. **152** (1966) 376.